Instantaneous Optimal State Feedback Control of Seismic Response using MR dampers

N. K. Chandiramani, S. P. Purohit

Department of Civil Engineering, Indian Institute of Technology Bombay
Powai, Mumbai-400076, INDIA

naresh@civil.iitb.ac.in, p7purohit@civil.iitb.ac.in

Abstract

Instantaneous Optimal Control is used to obtain desired force from MR damper fitted to a seismically excited building. Excitation is considered when minimizing performance index, unlike in classical optimal controllers. Modified Bouc-Wen damper model and on-off voltage law is considered. Various forms of state weighting matrix are considered for controller design. IOC is compared with LQR/LQG and PON control. It yields reduction in: maximum peak interstorey drift; and generally in accelerations vis-a-vis LQR/LQG. IOCSF Riccati Matrix Type controller appears most effective, yielding: lowest maximum peak drift/acceleration and generally best storeywise drift control vis-a-vis PON/LQR/LQG; substantially lower peak accelerations vis-a-vis LQR/LQG.

1. Introduction

Magnetorheological (MR) dampers are semi-active devices, using MR fluids having controllable yield characteristics, which produce sizeable damping force for small input voltage. Their hysteretic behavior can be represented using the modified Bouc-Wen model [1] having voltage dependent parameters. Various methods for controller design like LQR (Linear Quadratic Regulator), LQG (Linear Quadratic Gaussian) have been used with MR dampers [1, 2]. Due to the difficulty in inverting damper dynamics (i.e., obtaining voltage to produce a desired force), on-off type voltage law (Clipped Voltage Law (CVL) given by Dyke et al. [1]) is widely used in order to produce approximately the desired damper force from an MR damper. However, LQR/LQG algorithms do not consider external excitation during performance index (PI) minimization to derive optimal feedback control laws. Thus,

they result in sub-optimal control. Yang et al. [3] proposed Instantaneous Optimal Control (IOC) algorithms by including seismic excitation when minimizing the quadratic PI at each instant.

In this paper, IOC due to [3] is implemented for seismic response attenuation using an MR damper fitted to a building. The modified Bouc-Wen damper model is considered and a CVL is used. Various structures of state weighting (Q) that yield stable controllers are considered. Results are compared with LQR, LQG and PON control.

2. MR damper model, Voltage control law

The modified Bouc-Wen model [1], considered here, gives damper force f as

$$f = c_1\dot{y} + k_1(x - x_0) \tag{1}$$

$$\dot{y} = 1/((c_10 + c_11))\ \{\alpha z + c_10\,\dot{x} + k_10\,(x - y)\};\quad u' = \eta(u - \text{"v"}) \tag{2}$$

$$\dot{z} = -\gamma|\dot{x} - \dot{y}|z|z|^{n-1} - \beta(\dot{x} - \dot{y})|z|^n + A(\dot{x} - \dot{y}) \tag{3}$$

$$\alpha = \alpha_a + \alpha_b u;\ c_1 = c_{1_a} + c_{1_b} u;\ c_0 = c_{0_a} + c_{0_b} u; \tag{4}$$

Here x, $\dot{x}$ and f are damper displacement, velocity and force, respectively; z is the evolutionary variable describing hysteresis; u models the combined dynamics of current driver and delay in fluid reaching rhelogical equilibrium, and v is the control input voltage to current driver. Model parameters k_1, x_0, c_1, c_0, k_0, γ, β, A and n are as defined and given in [1].

The input voltage, v, to the damper is obtained using the CVL [1] as follows. If $f_d f < 0$ then $v = v_{min} = 0$ V; else $v = v_{max} = 2.25$ V when $|f_d| > |f|$ or $v = v_{min} = 0$ V when $|f_d| < |f|$, or v is held at its present value when $|f_d| = |f|$. Here f_d is desired damper force obtained from the controller and f is applied damper force.

3. Structural Model

A three storey test structure with single MR damper attached between ground and first storey [1] is used. The equation of motion is given as,

$$M_s\ddot{x} + C_s\dot{x} + K_s x = Gf - M_s L\ddot{x}_g \tag{5}$$

where M_s, C_s, and K_s are mass, damping, and stiffness matrices, respectively, G is the location matrix of MR damper, f is the applied control force defined by Eq. (1), L is the location matrix of earthquake excitation, $\ddot{x}_g$ is the ground acceleration (earthquake excitation), and $x = [x_1 \quad x_2 \quad x_3]^T$ is the displacement vector of the three storeys measured relative to ground. The data for the test structure is as given in [1]. The building is subjected to N-S component of the 1940 El Centro ground acceleration with time scale reduced fivefold. Defining $q = [x \quad \dot{x}]^T$ the state equations representing Eq. (5) are,

$$\dot{q} = Aq + Bf + E\ddot{x}_g \tag{6}$$

$$A = \begin{bmatrix} 0 & I \\ -M_s^{-1}K_s & -M_s^{-1}C_s \end{bmatrix};\ B = \begin{bmatrix} 0 \\ -M_s^{-1}G \end{bmatrix};\ E = -\begin{bmatrix} 0 \\ L \end{bmatrix} \tag{7}$$

4. Instantaneous Optimal Control

IOC algorithm considers the excitation in controller design unlike LQR control. Two such methods, suitable for structural control where excitation is not known apriori, are due to Yang et al. [4] (see also [5]) and briefly given as follows.

4.1 IOC with State Feedback (IOCSF)

In this method the state equations (Eq. (6)) are decoupled, using the eigensolution of A, and then solved using the state transition approach. Then, the PI $J^*(t) = q^T Q q + f^T R f$ is minimized at each instant, subject to the constraint Eq. (6) represented in terms of the state transition solution. This yields the closed loop control

$$f(t) = -\Delta t/2\ R^{-1}B^T Q q(t) \tag{8}$$

For control simulation, the state can be obtained by numerically integrating Eq. (6) or via the state transition solution (using Eq. (8)), i.e.,

$$q(t) = \left[I + \Delta t^2/4\ BR^{-1}B^T Q\right]^{-1}\left[Td(t-\Delta t) + \Delta t/2 E\ddot{x}_g\right] \tag{9}$$

where,

$$d(t-\Delta t) = \exp(\Lambda \Delta t)T^{-1}\left\{q(t-\Delta t) + \Delta t/2[Bf(t-\Delta t) + E\ddot{x}_g(t-\Delta t)]\right\} \tag{10}$$

Here T and Λ denote the modal matrix and diagonal matrix of eigenvalues of A, respectively. Note that, the effectiveness of IOCSF depends on the choice of time interval Δt and state weighting Q.

4.2 IOC with Velocity and Acceleration Feedback (IOC-VAF)

In this method PI $J(t) = q^T(t)Qq(t) + f^T(t)Rf(t)$ is minimized at each instant, subject to constraint Eq. (6) written using backward differencing ($q(t) = q(t-\Delta t) + \Delta t\, \dot{q}(t-\Delta t)$) so that $J(t)$ does not contain $\delta q(t)$. This yields the closed loop control

(11)

where $\dot{q}$ represents measured relative- velocities and accelerations. For control simulation, $\dot{q}$ is obtained from Eq. (6).

4.3 Q Structures and Implementation Issues

Yang et al. [4] proposed state weighting (Q) structures, using Lyapunov's direct method, which are summarized below. Here $\phi \equiv \Delta t/2$.

(1) IOCSF-Riccati Type Equation (IOCSF-RTE):

Choose $Q = \phi_1 Q_1$ where ϕ_1 is a positive constant and Q_1 is the solution of the Riccati type equation $A^T Q_1 + Q_1 A - 2\phi\phi_1 Q_1 B R^{-1} B^T Q_1 = -I_0$. Here, I_0 is a symmetric positive semidefinite matrix. Thus, choosing ϕ, ϕ_1, I_0, and R one obtains Q and the control from Eq. (8). Here $\phi = 0.002$, $\phi_1 = 23.15$, $I_0 = 10^3 I$, and $R = 10^{-10}$ is chosen for effective control.

(2) IOCSF-Riccati Matrix Type (IOCSF-RMT):

$Q = (\phi_2/\phi)P$ where ϕ_2 is a positive constant and P is the solution of the algebraic Riccati equation $PA + A^T P - PBR^{-1}B^T P = -I_0$. Thus, choosing ϕ, ϕ_2, I_0, and R one obtains Q and the control from Eq. (8). Here, $\phi = 0.002$, $\phi_2 = 0.0475$, $I_0 = I$, and $R = 10^{-11}$ is chosen for effective control.

(3) IOC-VAF:

Choose $Q = -A^T P^*$ where P^* is the solution of the Riccati type equation $A^T P^* + P^* A^{-1} - 2P^*(A^{-1}B)R^{-1}(A^{-1}B)^T P^* = -I_0$. Thus, choosing I_0 and R one obtains Q and the control from Eq. (11). Here I_0 is chosen as the null matrix except $I_{0_{33}} = 1$, and $R = 10^{-8}$ for effective control.

Another Q structure for IOCSF (IOCSF-Q_0): Since a single damper is fitted between ground and first storey only, for IOCSF it is readily concluded from Eqs. (7, 8) (see also G) that only the fourth row of Q contributes to the control input f. Thus, Q is chosen as the null matrix except for its fourth row which is $[Q_1 \;\; Q_2 \;\cdots\; Q_6]$ and the control obtained from Eq. (8). Here $Q_1 = Q_2 = Q_4 = Q_5 = 1, Q_3 = Q_6 = 2$, and $R = 10^{-8}$ is chosen for effective control.

Convergence studies using IOCSF-RM`T showed that $0.004 \leq \Delta t \leq 0.02$ yields effective control. Hence $\Delta t = 0.004$ is chosen in controller design. For results reported herein, controlled system dynamics is obtained by numerical integration of Eq. (6), with control input (i.e., desired damper force f_d) obtained from Eqs. (8, 9), and CVL is used to obtain applied damper voltage. Note that in IOC-VAF the relative velocities and relative accelerations are fed back. However, since absolute accelerations are readily measured, an ad-hoc modification (i.e., IOC-VAFM) involving feedback of relative velocities and absolute accelerations is considered whereby relative velocities are obtained using Eq. (6) and absolute accelerations are obtained as $Cq + Df$, where $C = [-M_s^{-1}K_s \quad -M_s^{-1}C_s]$ and $D = [M_s^{T}G]$.

5. Results and Discussion

The following cases are considered: (1) Passive Control: For passive-on (PON) case the damper saturation voltage $v = 2.25\ V$ is applied. (2) Semi-active Control (SA): Desired damper force f_d is determined using IOCSF (or LQR/LQG for comparisons). For LQR, $Q = I$ (identity matrix) and $R = 10^{-11}$ is chosen for effective control. For LQG, $Q = \hat{C}^T\hat{Q}\hat{C}$, where $\hat{C} = [C^T \vdots [1 \ 0 \ 0 \ 0 \ 0 \ 0]^T]^T$ and $\hat{Q}$ is the null matrix except $\hat{Q}_{33} = 1$, i.e., only top storey acceleration is weighted, and $R = 10^{-17}$ [1].

The system of Equations (2), (3), (6) are integrated using MATLAB ODE45 ($\frac{4^{th}}{5^{th}}$ order Runge - Kutta method) for zero initial conditions. Peak response (i.e., storeywise- interstorey drift ($x_{i-1} - x_i$), displacement, acceleration, and damper force) and PI are obtained. For easy comparison, the PI for PON control is calculated using the same Q and R as the corresponding semi-active PI. Here, maximum peak refer to the storeywise maximum of the particular response quantity.

Comparison of IOCSF and PON control

IOCSF achieves substantial reduction in maximum peak drift vis-a-vis PON control, i.e., 29% using IOCSF-RMT; 28% using IOCSF-RTE; 28% using IOCSF-Q_0; 19% using IOC-VAF; and 25% using IOC-VAFM. IOCSF shows storeywise reductions, except for damper storey, of at least: 12% (IOCSF-RTE, storey-3) and 7% (IOCSF-Q_0, storey-2) for peak- drift and displacement, respectively. The peak damper force applied is higher (by $< 6\%$) for IOCSF-RTE/IOC-VAF and lower ($> 3\%$) for IOCSF- RMT/Q_0/IOC-VAFM. The PI is lower for IOCSF, except for IOCSF-Q_0.

Comparison of IOCSF and LQR

IOCSF yields a reduction of up to 12% in maximum peak drift vis-a-vis LQR, with IOCSF-RMT yielding the highest reduction. The storeywise peak drift also

shows a reduction, except at damper storey, of up to 20% (IOCSF-RMT, storey-2). Storeywise peak accelerations are also mostly lower, the reduction being up to 35% (IOC-VAFM, storey-1). However, storeywise peak displacements are mostly higher (up to 15%). Peak values of damper force reduce up to 16% (IOCSF-$Q_1 0$).

Comparison of IOCSF with LQG

The maximum peak drift resulting from IOCSF is comparable, lying between -6% and 5% of the LQG result. Storeywise peak accelerations from IOCSF are mostly reduced, the highest reduction being 38% (IOCSF-Q_0, storey-2). Peak damper forces from IOCSF lie within -12% and 5% of the LQG values.

Comparison amongst IOCSF controllers

Figure 1 shows the comparison of IOCSF controllers, for storeywise peak responses (i.e., drift, displacement, and accelerations). This shows that: IOCSF-Q_0 yields the best drift control, followed by IOCSF-RMT (Fig. 1(a)); all IOCSF controllers provide comparable displacement control (Fig. 1(b)); IOC-VAFM yields the best acceleration control, followed by IOCSF-RMT (Fig. 1(c)). Except IOCSF-Q_0, all IOCSF controllers yields PI lower than the corresponding PON value (reduction being between $29-35\%$). Comparison of IOC-VAF and the ad-hoc IOC-VAFM controllers shows that the latter provides substantial reduction in drift and acceleration while displacements are comparable. Considering all response quantities and PI reduction, IOCSF-RMT appears most effective amongst IOCSF controllers. Henceforth it is used for comparison with PON, LQR and LQG.

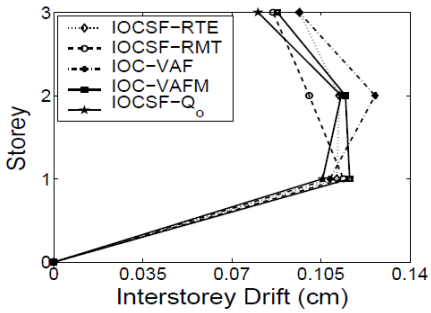

(a)

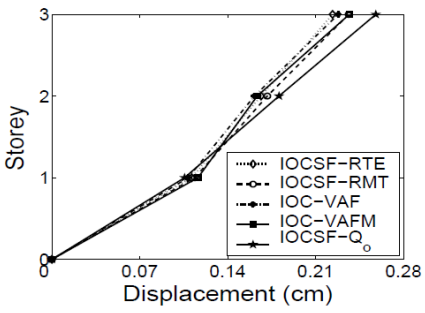

(b)

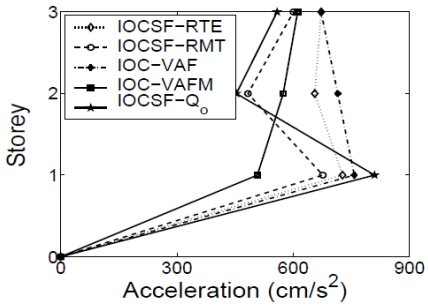

(c)

Fig. 1. Storeywise peak response, IOC controllers (a) interstorey drift (b) displacement (c) acceleration

Comparison of IOCSF-RMT with PON, LQR and LQG controllers

Figure 2 shows the comparison of IOCSF-RMT with PON, LQR, LQG control, for storeywise peak responses. Figure 2(a) shows that IOCSF-RMT provides the lowest maximum peak drift (compare maximum peak drift occurring at- storey-1 for IOCSF-RMT and LQG, storey-2 for LQR and PON) and it generally has the best storeywise performance. While PON control provides the lowest peak drift at damper storey, it is least effective at the remaining storey's, and is outperformed by semi-active controllers as they attempts to keep the drift uniformly low at all storeys.

Figure 2(b) shows that peak displacements from IOCSF-RMT lie between LQR and LQG values except at the top storey where the maximum peak displacements occur. Thus IOCSF-RMT yields the highest maximum peak displacement amongst semiactive controllers. While PON control provides the lowest peak displacement at damper storey, it is least effective at the remaining storeys, and is generally outperformed by semi-active controllers.

Figure 2(c) shows that IOCSF-RMT clearly outperforms LQR and LQG controllers by yielding substantial reductions in storeywise peak acceleration, and it also yields the lowest maximum peak acceleration amongst all controllers (compare maximum peak acceleration occurring at- storey-1 for IOCSF-RMT, LQR, LQG, storey-3 for PON). While PON control clearly provides the lowest peak acceleration at damper storey, it yields the highest maximum peak acceleration. It is interesting to note that although LQG attempts to minimize a PI based on only top storey acceleration, it generally has the poorest performance in acceleration control. This may be due to the greater flexibility available in choice of weighting matrices $\boldsymbol{Q}$ and $\boldsymbol{R}$ when applying LQR and IOC-RMT control.

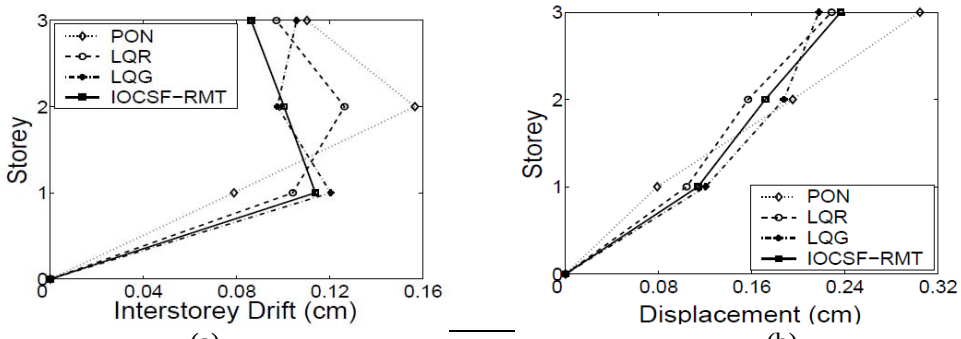

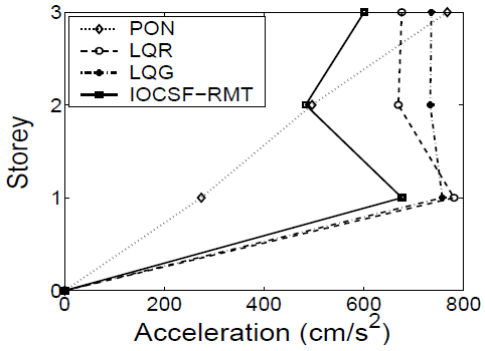

(c)

Fig. 2. Storeywise peak response, PON, LQR, LQG, IOCSF-RMT controllers (a) interstorey drift (b) displacement (c) acceleration

6. Conclusions

Instantaneous optimal control is used to determine the desired force required from an MR damper attached between ground and first storey of a seismically excited building. A modified Bouc-Wen damper model and an existing CVL are used. The performance of various IOC controllers are assessed and compared with PON, LQR and LQG control. The significant conclusions are:

(1) IOC provides mostly a reduction in maximum peak drift, although not a storeywise drift reduction. Accelerations are generally reduced vis-a-vis other semi-active controllers.

(2) A comparison of IOC-VAF and the ad-hoc IOC-VAFM controllers shows that the latter provides substantial reduction in drift and acceleration with comparable displacements.

(3) IOCSF-RMT appears most effective amongst IOC controllers. When compared with PON, LQR, LQG, it provides the lowest maximum peak drift and generally the best storeywise drift performance also. It outperforms LQR and LQG controllers in terms of storeywise peak acceleration, and yields the lowest maximum peak acceleration amongst all controllers. However, it marginally yields the highest maximum peak displacement amongst semi-active controllers.

References

1. Dyke S.J., Spencer B.F. Jr., Sain M.K. and Carlson J.D. (1996), Modelling and Control of Magnetorhelogical Dampers for Seismic Response Reduction, Smart Material and Structure, vol. 5, pp. 565-575.
2. Chang C.C. and Zhou L. (2002), Neural Network Emulation of Inverse Dynamics for a Magnetorhelogical Damper, ASCE Journal of Structural Engineering, vol. 128,pp. 231-239.

3. Yang Y.N., Akbarpour A. and Ghaemmaghami P. (1987), New Optimal Control Algorithms for Structural Control, ASCE Journal of Engineering Mechanics, vol. 113,pp. 1369-1386.
4. Yang Y.N., Li Z. and Liu S.C. (1992), Stable Controllers for Instantaneous Optimal Control, ASCE Journal of Engineering Mechanics, vol. 118,pp. 1612-1630.
5. Soong, TT. (1990), Active Structural Control: Theory and Practice. 1^{st} edition, Longman Scientific & Technical, England, pp 36-40.

Time history comparison

Figure 3(a) shows time trace of voltage applied to the damper when using IOCSF-RMT control. The voltage switches between $v = 0\ V$ and $v = 2.25\ V$ levels, remaining saturated for 34% of total simulation time shown. Thus IOCSF-RMT affords tremendous power savings vis-a-vis PON control. Time traces of desired and applied damper forces are compared in Fig. 3(b). Differences between applied and desired damper forces are apparent. These are due to (i) inverse dynamics of damper being difficult to obtain, due to which CVL is considered; (ii) damper force saturating at $v = 2.25\ V$, which limits the maximum force that the damper can produce; (iii) damper constitutive law that restricts force-velocity plot to lie in first and third quadrants despite desired damper force, obtained by IOCSF-RMT, traversing all quadrants. The applied damper force (f) appears to follow desired damper force (f_d) reasonably well, thus justifying use of the CVL to command the MR damper.

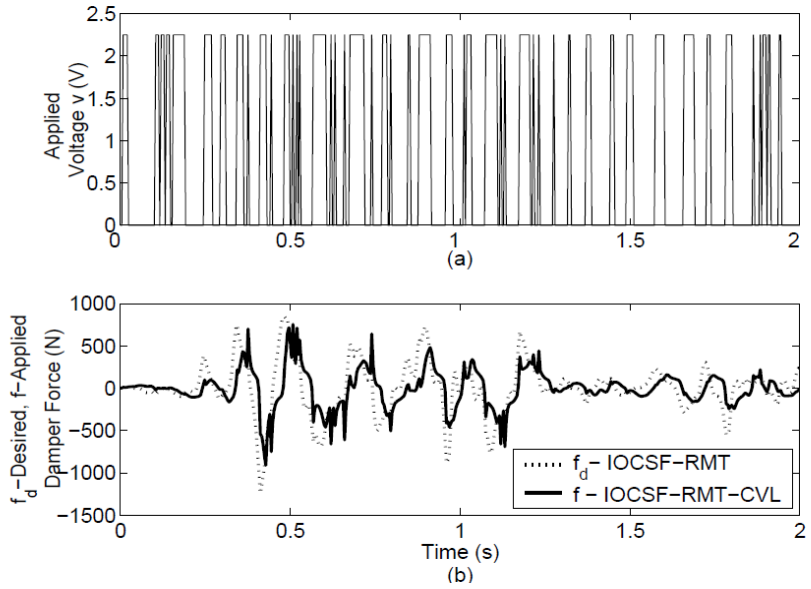

Fig. 3. Time histories (a) Applied voltage (b) Desired-, Applied- damper force; IOCSF-RMT